Wind-terrain effects on the propagation of large wildfires in rugged terrain: fire channelling

J.J. Sharples[1,2], R.H.D. McRae[2,3], R.O.Weber[1,2] and S.R.Wilkes[4]

1. School of Physical, Environmental and Mathematical Sciences, University of New South Wales at the Australian Defence Force Academy. Canberra, ACT, Australia.
2. Bushfire Cooperative Research Centre. East Melbourne, Australia.
3. ACT Emergency Services Agency. ACT, Australia.
4. Fire Management Unit. ACT Parks, Conservation and Lands. ACT, Australia.

Draft: 24 June 2009

Abstract

The interaction of wind, terrain and a large fire burning in a landscape can produce a variety of unusual yet significant effects on fire propagation. One such example, in which a fire exhibits rapid spread in a direction transverse to the ambient winds as well as in the usual downwind direction, is considered in this paper. This type of fire spread is characterised by intense lateral and downwind development of spot fires, the production of zones of deep flaming and bidirectional fire spread. By appealing to the theory of dynamic channelling and utilising wind, terrain and multispectral fire data collected during the January 2003 alpine fires over southeastern Australia, we present an argument that supports the hypothesis that this type of fire spread is associated with particular elements of the terrain that align with the ambient winds in a certain way; incised valleys and steep lee slopes are found to be particularly important. Given the apparent connection to channelling of air flows by complex terrain, this type of fire spread is referred to as 'fire channelling'. A two-parameter terrain-filter model is developed to quantitatively confirm the exclusive link between fire channelling and steep parts of the landscape that are lee-facing. The model is then used to identify parts of the landscape prone to the occurrence of fire channelling, information that can then be used to inform operational decisions as well as planning and policy development. The model is shown to give necessary conditions that the wind and terrain must jointly satisfy in order for the fire channelling phenomenon to occur. These conditions are found to be insufficient, however. Conditions of sufficiency are briefly discussed along with the implications of channelling-driven fire spread for bushfire risk management.

1. Introduction

The January 2003 alpine fires in southeastern Australia were memorable in many ways. In particular, under extreme weather conditions on the afternoon of 18 January, fires that had originated to the west of Canberra as a number of separate fires, merged and impacted on the national capital (Nairn, 2003). In the resulting firestorm four lives were lost and hundreds of houses were destroyed within a few hours. The Canberra fires also stand out as some of the best documented wildfires in Australia. The fires were documented in the form of airborne and land-based photographs and video, satellite data, including photographs by astronauts, and fire data that was recorded by a multispectral line-scanning instrument fitted to an aircraft that flew several missions over fire affected regions. These data sources permit analyses of the extreme fire behaviour experienced during the event. Additional insight is obtained from similar material gathered after the fires, recording the severity of impact on the landscape. Analyses of the fire behaviour experienced around Canberra on the afternoon of 18 January have identified a number of processes associated with the extraordinary intensity of the fires. For example, Dold et al. (2005) describe a range of unusual combustion processes identified from eye witness accounts, Fromm et al. (2006) discuss the extreme convection created by the fires, Mills (2006) discusses the link between the extreme fire behaviour and the passage of a potentially forecastable region of dry upper air over the fire and Mitchell et al. (2006) discuss the smoke generated by the fire and its effects on subsequent weather. A review of the general meteorology surrounding the event is given by Taylor and Webb (2004).

The terrain to the west of Canberra is dominated by the Brindabella Ranges, which are a sequence of rugged mountain ridges and valleys that are aligned roughly in a north-south direction. Given the complex terrain in which the fires were burning and the strong winds experienced during their most devastating runs towards Canberra, it is natural to consider the concept of wind-terrain interaction and to investigate what significance interactions between the wind and the terrain may have had on the development of the fire. Wind-terrain interactions, which refer to the way that properties of the fluid air (the wind) are affected by terrain features, can occur over a variety of spatiotemporal scales depending on the atmospheric structure, characteristics of the ambient wind flow and the details of the topography.

Macroscale examples of wind-terrain interaction (alternatively termed atmosphere-terrain interactions at this scale) include mountain wind waves and foehn flows (Barry, 1992; Whiteman, 2000) and involve interaction of large air masses with broad scale topographic features such as mountain ranges. Mesoscale wind-terrain interactions include phenomena such as flow separation in the lee of mountain ridges, thermal winds and dynamic channelling of air flows along mountain valleys (Whiteman, 2000). It is important to note however, that even with mesoscale processes such as dynamic channelling further scale divisions can be identified with respect to the driving processes. Pressure driven channelling is mainly responsible for modification of large scale winds in broad and long valleys (Wippermann and Gross, 1981; Whiteman and Doran, 1993), whereas forced channelling mainly occurs in smaller valleys, mountain passes or saddles (Weber and Kauffmann, 1998). A study by Smedman, et al. (1996) on intermediate

valleys suggests that both pressure-driven and forced channelling processes can occur in combination. Microscale examples of wind-terrain interactions include winds driven by thermal or frictional differences in small-scale terrain features such as gullies, and turbulent eddies that form as winds of sufficient strength flow around prominent peaks and hills or over sharp ridges.

Understanding how local and regional winds can be modified through microscale and mesoscale wind-terrain interaction is an important problem when attempting to model the propagation of wildfires in complex terrain. Unexpected changes in wind direction and strength have been linked with several incidents where experienced fire fighters working in rugged terrain, have been killed or injured due to a sudden escalation in the severity of fire behaviour (Rothermel, 1993; Butler et al., 1998; Cheney et al., 2001; Rothermel and Brown, 2003; Butler et al., 2003).

In this paper we identify a number of features in the multispectral line-scan data collected on the afternoon of 18 January that suggest a link between unusual fire propagation and parts of the terrain that align with the prevailing winds in a certain way. By appealing to the theory of mesoscale wind-terrain interactions, in particular flow separation and channelling theory, we propose some processes that could account for the unusual fire propagation, and derive a terrain-filter model that identifies regions of the landscape prone to the types of processes captured in the line-scan data. The model can be assessed and refined by appealing to further fire data, including multispectral line-scan datasets as they become available.

We begin by discussing the concepts of dynamic channelling and flow separation in greater depth in section 2, before detailing the characteristics of the various datasets used in the study in section 3. In section 4 we introduce a terrain-filter model, which is used to identify regions of the landscape prone to the unusual fire behaviour. The model is calibrated using a subset of the line-scan data (three events) in section 5 before being validated on several other events.

2. Dynamic Channelling

Channelling is a particular type of wind-terrain interaction that can occur whenever certain terrain features align in a particular way with the geostrophic wind direction. Incised valleys and gaps between mountains can have winds diverted along or between them in response to local differences in friction or pressure (Whiteman and Doran, 1993; Kossmann et al., 2001). Forced channelling results when the valley side-walls cause frictional differences which are much less in the along-valley direction than they are in the across-valley direction. This frictional difference forces the wind to align preferentially along the valley axis, with the strength and direction of the channelled flow dependent upon the sign and magnitude of the component of the ambient winds relative to the valley axis. This implies that, under ideal conditions, the induced valley winds can undergo an immediate change in direction of 180^{o} as the ambient wind direction changes across a line perpendicular to the valley axis (Doran and Whiteman, 1992; Whiteman and Doran, 1993; Kossmann, et al., 2001; Kossmann and Sturman, 2002). Pressure-driven

channelling occurs when the air within a valley responds to the component of the geostrophic pressure gradient along the valley axis (Fiedler, 1983). This effect would be more pronounced when the upper winds separate from the surface and pass over the valley, allowing the air within the valley to move almost independently of them. In contrast to forced channelling, valley winds arising from pressure-driven channelling will switch direction by 180^{o} whenever the ambient wind direction crosses a line parallel to the valley axis. Consequently, counter-currents can occur, which flow in opposition to the main component of the ambient winds (Wippermann and Gross, 1981; Wippermann, 1984; Gross and Wippermann, 1987; Kossmann and Sturman, 2003).

When the geostrophic winds are strong, airflows resembling dynamic channelling can also occur in the lee of mountain ranges, even without the presence of a definite valley. Under such circumstances the winds can be forced up and over the ridge resulting in separation of the flow from the surface in the lee of the ridge. The separation of the geostrophic and the near-surface winds in the lee of the ridge line can lead to the formation of a lee-slope or separation eddy (Lee et al., 1981; Byron-Scott, 1990, Papadopoulos et al., 1992). These horizontal axis eddies can extend along the entire length of the ridge (Whiteman, 2000). The partial decoupling of the near-surface winds and the upper winds in the lee of ridge lines also permits the generation of local winds that can flow with an across-slope component along the lee slope with a speed and direction dictated by the across-slope component of the ambient winds, local pressure gradients or thermal influences. The net effect is for the air to follow a helical pattern about a horizontal axis aligned approximately parallel to the ridgeline. This phenomenon could be termed lee-slope channelling (McRae, 2004).

The effect that dynamic channelling might have on fire propagation and smoke dispersal is discussed in Kossmann et al. (2000). The direction of channelling-driven winds within a valley can often be quite different, sometimes even perpendicular or opposed, to the ambient wind direction. The wind direction within valleys prone to dynamic channelling is often stable with respect to changes in the ambient wind direction unless these changes occur near some threshold wind direction. If the ambient winds change direction across some threshold value, however, then as mentioned above, the channelling driven winds within the valley can rapidly change direction by 180^{o}. The threshold wind direction is dependent upon whether the channelling is forced or pressure-driven. The role that channelling played in the Canberra fires was first identified as a problem worthy of further research by McRae (2004), who identified forced and lee-slope channelling as likely processes driving the severe fire growth.

3. Data and Methods

3.1 Wind and Terrain Data

Two sets of wind data for 18 January 2003 were obtained: the first from the Bureau of Meteorology (BoM) automatic weather station located at Canberra Airport, and the second from an automatic weather station located at the Emergency Services Bureau Headquarters at Curtin, approximately 10 km west of Canberra Airport. Wind speeds

averaged around 30-40 km h^{-1} during the worst of the fire activity, reaching a maximum of just under 50 km h^{-1} at 15:30. Wind gust reached a maximum of just under 80 km h^{-1} at approximately the same time. The wind direction contributing to the most devastating fire runs varied between west-northwest and northwest. After 19:00 the winds shifted to the southeast in association with a cool 'sea breeze' change (Webb et al., 2004; Mills, 2005; Taylor and Webb, 2005; Taylor et al., 2005). Figure 1a shows wind data recorded at Canberra Airport on 18 January 2003, while figure 1b shows the wind data recorded at Curtin for the same period.

Terrain data for the region of interest is derived from the 90 metre resolution Shuttle Radar Topography Mission data (Farr et al., 2007). This digital elevation model (DEM) was rescaled to 250m resolution and was used to derive gridded slope and aspect data within the GIS software MapInfo Professional™.

3.2 Multispectral Linescan Data

Multispectral scanners are a particular class of remote sensing device that sense radiation in multiple wavelength regions of the visible, near infrared, middle infrared and thermal infrared parts of the electromagnetic spectrum. Radiation received by a multispectral scanner is recorded in a number of distinct spectral bands (Harrison and Jupp, 1989).

The Daedalus 1268 airborne thematic mapper (ATM) instrument collects radiance measurements in 10 spectral bands covering the visible and near-infrared spectrum from 0.45μm to 1.05μm and two thermal-infrared bands (high and low gain) covering the 8.5μm to 13μm spectrum. Of the twelve bands, eight are used to discriminate land surface features and correspond to Landsat Thematic Mapper TM bands. Data is collected as digital numbers representing radiance on a scale of 0 to 255 (8-bit) with an instantaneous field of view (IFOV) of 1.25 milliradians across 42.5^{o} swathes (716 pixels per scan line) in band interleaved by line (BIL) format. Inertial navigation system (INS) data is stored in a thirteenth band, recording geographic position in addition to the pitch, roll and yaw of the aircraft platform for each line. The INS band is used to fully orthorectify the data over a digital elevation model. This provides a 'real-world' representation of the imagery. During the 2003 fires the orthorectification was done using XQinertia™ software. Characteristics of the spectral bands for the Daedalus 1268 ATM instrument are presented in Table 1 (Harrison & Jupp, 1989).

During the 2003 alpine fires a Cessna 404 carrying a Daedalus 1268 ATM was tasked to fly parallel traverses of the fire complex to the west of Canberra. The device was flown at approximately 6500m during the missions on 18 January 2003, yielding a sensor footprint (pixel size) of around 7m×7m at nadir. Starting at 14:29ADST on the outskirts of Canberra, the mission was completed after nine scan runs concluding at 15:57ADST to the west of the Brindabella Valley. Note that ADST (Australian Daylight Savings Time) is UTC+11 hours. Due to the rapid escalation of the fires, the nine runs were of limited operational use but were used to establish mid-afternoon fire perimeters and to make sense of the impact on the Canberra suburbs. The orthorectified data were georectified to correct for the relativity of the flight path to the underlying complex topography. No formal ground control points were used. Some data processing was conducted to create a

standard operational image set for bushfire managers (Cook *et al.*, 2006). Limited overlap exists between runs, which allowed some information on the temporal development of the fire to be gleaned from the data.

Interpretation of line-scan data of dynamic events such as bushfires can disclose a significant amount of information. While the data represent snapshots of time with limited spatial overlap across various time periods, knowledge of fire behaviour can indicate trends across the landscape when considering time dependent events such as combustion and its decay-persistence times. Flaming combustion depth can indicate rate of fire spread in a comparative way or, with overlapping runs, in an absolute sense. Post-event line-scans can be used give an indication of impact on biota and soil chemistry.

The key to understanding the colours in the line-scan imagery is the mapping of the three spectral bands 3 (green), 5 (red) and 8 (near infrared) onto the three-dimensional RGB colour system. The additive rendering of a colour is based on intensity for each of the three channels ranging from 0 (dark) to 255 (full intensity). The processing of the images is intended to give key features a consistent pseudo-colour, so that a trained observer may easily interpret the imagery. The majority of the spectral signatures relating to fire behaviour can be identified with portions of the RG plane (i.e. B = 0), while remaining spectral signatures, such as those corresponding to vegetation and bodies of water, need to be interpreted using the full RGB cube. Table 2 shows indicative RGB coordinate values for features within an image with a well balanced pixel intensity distribution. Flames do not emit strongly in the near IR band used 910 – 1050 nm. As a result very few pixels lie on the grey trend line between white and black, enhancing the value of pseudo-colour hue in image interpretation.

Close examination of the line-scan data collected on 18 January revealed a number of interesting events. The locations of three of these events are indicated by large dots in figure 2a and are illustrated in more detail in figure 2b. The following subsections provide more detail on these three events. Locations of other significant events in southeastern Australia are indicated by the small dots in figure 2a, and are listed in table 3.

3.2.1 Bendora Dam

Bendora Dam is located approximately 32 km southwest of Canberra and is surrounded by rugged terrain (figure 2b). The Bendora Fire had been burning to the northwest of Bendora Dam since its ignition by a dry lightning storm on 8 January. In the early afternoon of 18 January a small unburnt patch on the edge of the Bendora Fire flared up. It is clearly seen as the orange area, circled in figure 3a. Figure 3b shows the same area 46 minutes later. Winds were from the west-northwest. Figure 3 shows the fire developing downwind as would be expected, but also indicates lateral development. Figure 3 indicates that in 45 minutes the fire exhibited a lateral spread of approximately 4km. This corresponds to a lateral spread rate of around 5.5 km h^{-1}. The direction of spread is almost due south, approximately perpendicular to the ambient wind direction.

Close examination of figure 3 reveals some interesting features. The flaming zone consistently extends downwind for at least 5 km with a uniform spectral signature in the imagery. The southern edge of the flaming zone consists of an edge aligned with the ambient winds, comprising many spot fires growing and amalgamating. On its upwind (western) edge the flaming zone is constrained by a major break in slope. This break follows the rim in the lower incised valley.

It is interesting to note that extrapolating backwards in time and assuming a constant rate of lateral spread, the fire would have only covered approximately 10 ha at 14:00.

3.2.2 Flea Creek

The location of Flea Creek can be seen in figure 2. Flea Creek runs north to south below a steep east-facing slope. Flea Creek meets the Goodradigbee River, which runs south to north along an incised valley of 300-400m relief.

Prior to 18 January a fire had been burning in the upper right quadrant of figure 4a for some days, and was contained east of the Goodradigbee River (figure 2b). A spot over occurred late on 17 January and was not contained. With the arrival of extreme weather conditions on 18 January, the fire spread southwards along the incised river valley. Ultimately it reached a point where the fuel downwind of the fire was unburnt, and the fire's behaviour escalated rapidly. Photographs of the convection column and radar data suggest that this was the most intense fire event of the day. The overlapping line scans do not allow calculation of a lateral spread rate; however, they do permit the following observations. The downwind development of the flaming zone is of the same scale as that for the Bendora event. There is extensive development of spot fires around the new fire edge, to the south and to the east. The upwind, westerly edge of the fire is constrained downwind of the break in slope atop the incised lower valley.

3.2.3 Broken Cart

The location of the Broken Cart event can be seen in figure 2. The northern edge of the fire perimeter, seen in figure 5b, displays a distinct kink where the fire appears to have propagated rapidly in a north-northeasterly direction. The region downwind of this part of the fire perimeter displays a uniform spectral signature over a distance of approximately 5 km. This region of deep flaming is constrained on its upwind edge by a break in topographic slope. Several spot fires can be seen burning to the north of this flaming zone, despite the fact that the ambient winds were from the west-northwest.

The southern edge of the fire in figure 5 displays similar behaviour. Here the fire appears to have rapidly propagated in a south-southwesterly direction, resulting in a distinctly right-angled fire perimeter. Downwind of this part of the perimeter the fire displays a uniform spectral signature in the imagery for at least 2 km (up to the extent of the image) indicating an expanse of deep flaming. The upwind edge of this region roughly coincides with a ridge line. A number of spot fires can be seen to the south of the region of deep flaming, forming in a direction that is transverse to the ambient winds. The fire behaviour evident in this part of the image is in stark contrast to that seen on the southern flank, upwind of the zone of deep flaming.

4. A model for identifying channelling prone regions

In the three cases considered in the last section a number of common features were evident. In particular, each case was characterised by rapid lateral propagation of the flank along a valley or lee-slope; downwind extension of the flaming zone of 2-5 km with uniform spectral signature in the imagery; the upwind edge of the flaming zone was constrained by a major break in topographic slope; and one edge of the flaming zone was roughly aligned with the ambient wind direction and was comprised of many spot fires. The fact that, in all cases, the upwind edge of the flaming zone coincided with a major break in slope indicates that the interaction of the strong ambient winds with the rugged terrain played a central role in the unusual fire propagation observed on 18 January. To account for the features seen in the line-scan data a simple terrain-filter model was developed. The model is based on wind direction and topographic slope and aspect and is intended to distinguish those parts of the landscape that are susceptible to the type of lateral fire spread discussed above.

Interactions between the wind and terrain, causing the type of fire behaviour discussed above, will also depend on the strength of the wind and the stability of the atmosphere (Sharples et al., submitted) but these factors will not be considered in these initial analyses. The terrain-filter model could potentially be refined and extended to include these factors as more information from other large fires in rugged terrain becomes available.

The terrain-filter model takes the form of a characteristic function as follows:

$$\chi(\sigma,\delta) = \begin{cases} 1 & \text{if } \gamma_s \geq \sigma \text{ and } \left|\theta_w - \gamma_a\right| \leq \delta, \\ 0 & \text{otherwise.} \end{cases} \qquad (1)$$

Here γ_s is the topographic slope angle, γ_a is the topographic aspect and θ_w is the direction that the ambient wind is blowing towards (i.e. the standard wind direction ± 180^o). The model is defined by the parameters σ and δ, which denote a threshold topographic slope angle and a threshold difference between the wind direction and topographic aspect, respectively. In plain terms, the model identifies parts of the landscape steeper than σ and with a topographic aspect within δ of the ambient wind direction (modulo 180^o).

5. Results

Using a geographic information system (MapInfo^{TM}) equation (1) was applied over the digital elevation model. The resulting grid (of 0's and 1's) was then compared to fire perimeter data derived from the line-scan imagery (figure 6). By varying the parameters σ and δ in the model we sought to produce a grid that matched well with those parts of the landscape where the unusual fire spread occurred. The model was thus calibrated by varying the parameters by hand until we obtained the smallest subset of the landscape that contained all the locations identified in the three events discussed above.

Assuming a west-northwesterly ambient wind (θ_w = 112.5^o) over the three regions of interest the calibrated model parameter values were found to be σ = 10.5^o and δ = 33^o. Hence the calibrated model identifies parts of the landscape with topographic aspects between 79.5^o and 145.5^o and with topographic slopes above 10.5^o. Note that the derived threshold slope value σ = 10.5^o relates to a DEM of 250m resolution. Converting this to a value in terms of actual topographic slope, using the scaling formula of McRae (1997), we obtain a value of $\sigma^* \approx 36^o$.

Figure 6 illustrates the output of the model as it compares to the fire perimeter data for the Broken Cart fire. The outlined regions in figure 6 are those parts of the landscape where unusual fire spread was identified. The model identifies the outlined regions but also identifies parts of the landscape with similar slope and aspect. As can be seen in figure 6, the Broken Cart fire passed over some of the regions identified by the model without displaying unusual fire spread (e.g. southern flank upwind of the outlined region). This means that the model identifies a condition of the landscape that is necessary for the type of unusual fire spread discussed in the three events, but that is not sufficient. Conditions of sufficiency would also likely include non-topographic factors such as fuel structure, load and moisture content as well as ambient wind speed and within-stand (microscale) atmospheric dynamics, including vertical airflow.

The results suggest that the unusual fire behaviour (lateral spread and spot fire development, intense down wind spotting) is caused by an interaction between the fire and the local (terrain-modified) winds. The model identifies two terrain types: incised valleys and steep lee slopes. In these terrain types channelled flows and lee-slope eddies are not uncommon, particularly in stronger winds such as were experienced on 18 January (Sharples et al., submitted). We will refer to this interaction as 'fire channelling'. Each of the events discussed in sections 3.2.1-3.2.3 can thus be termed either a 'lee-slope' or 'valley channelling event'.

After calibration the model was tested by comparing its output to other parts of the landscape where similar unusual fire spread was observed. These included events during the Canberra fires as well as the Thredbo fires, which occurred on 26 January 2003. The events that took place in the Thredbo Valley can be seen in the multispectral line-scan imagery of figure 7. Figure 7a shows the rectified line-scan data overlayed on a shaded digital elevation model of the Thredbo Valley. Three events characterised by lateral fire spread and spot fire development can be seen in the centre and left of the figure. In figure 7b the line-scan data is again shown, but as a semi-transparent layer so that the output of the terrain-filter model can be seen. The regions identified by the terrain-filter model are indicated by grey grid cells in figure 7b. Figure 7b shows that the parts of the fire exhibiting lateral spread and intense behaviour are anchored at or near a piece of the landscape identified by the terrain-filter. The model parameters used to construct the grid seen in figure 7b were the same obtained through calibration of the model using the Broken Cart, Bendora Dam and Flea Creek events of 18 January 2003. The terrain-filter model was also applied to several other fire channelling events, identified using multispectral line-scan data or aerial photography, and was found to consistently identify

parts of the landscape where the unusual fire spread was observed. A list of all the channelling events known to the authors is given in table 3. The locations of the Australian events listed in table 3 are also indicated by the small dots in figure 2a.

The success of the terrain-filter model in consistently identifying parts of the landscape where the unusual fire spread was observed is a strong indication that the phenomenon is caused by the interaction of the fire, the wind and steep, lee-facing terrain. Based on the observations and the model analyses it is possible to propose a mechanism that accounts for the unusual channelling-like fire spread. Figure 8 illustrates the hypothetical mechanism for the separate cases of an incised valley (figure 8a) and a steep lee slope (figure 8b). In each case an eddy-like structure forms within the incised valley or across the lee-slope, due to separation of the ambient flow from the terrain surface. Once a bushfire enters a region prone to eddy formation, the fire can act to intensify the vortical flow (Byron-Scott, 1990) and the increased turbulence can facilitate more efficient production of embers, which are then circulated with the eddy. The observations then suggest that these embers can move in a lateral direction, igniting spot fires in a direction transverse to the main wind direction. This lateral spread could occur through a number of processes, but thermal gradients due to the presence of a large fire would appear to be an important driving factor. In addition to their advection by the lateral flow, a proportion of the embers are 'peeled off' by the strong ambient winds and are deposited downwind where they ignite further spot fires that grow and amalgamate. The bidirectional nature of the process, with embers advected both laterally and downwind, means that it can rapidly and efficiently spread a fire across a landscape. The result of the process is an extensive region of deep flaming, which can in turn lead to pyro-cumulonimbus development and the transition to a plume-driven fire.

6. Discussion and Conclusions

A number of instances of unusual fire behaviour have been presented and discussed. These instances involved rapid, bidirectional fire spread transverse to, as well as in the direction of the ambient winds, the lateral development of spot fires and the formation of regions of deep flaming downwind. Examination of these types of events consistently revealed an association with certain terrain features, such as major breaks in steep lee slopes or incised valleys. Based on these observations a terrain-filter model was introduced. The model, which took the form of a parameter-dependent characteristic function, was shown to consistently identify conditions necessary for the type of fire spread described. The model confirmed the connection between unusual fire spread and steep lee slopes or incised valleys; the interaction of the fire, the slope and the terrain-modified flow result in a phenomena that could be termed 'fire channelling'.

The observations and success of the model suggest the following rationale for the unusual fire spread in the Bendora Dam, the Flea Creek and Broken Cart events. The Bendora event involved channelling-driven fire spread in a southerly direction along the Bendora valley. Similarly the Flea Creek event involved southerly spread driven by channelling along the Goodradigbee Valley. The Broken Cart event involved progression of the fire

along steep lee slopes in both northerly and southerly directions driven by the interaction of the fire with a lee slope eddy. The other events listed in table 3 can be accounted for by similar arguments.

While the terrain-filter model was able to identify regions or terrain conditions that were necessary for the fire channelling process to occur, these terrain conditions were not sufficient. For example, there were a number of instances where fire burnt over a region identified by the terrain-filter model without any evidence of fire channelling. Conditions of sufficiency are also likely to include factors such as fuel moisture, fuel structure and fuel load. The capability of the fire-channelling process to rapidly spread a fire across a landscape is dependent upon the rate at which spot fires ignite, spread and amalgamate. Hence, fire channelling events will be more likely in high fuel loads, in fuels that are conducive to ember formation (e.g. stringy bark) and when fuel moisture contents are very low. Anomalously low fuel moisture content was certainly a feature of all the events listed in table 3. Sharples et al. (2009) have shown that the quantity $T - H$, where T is air temperature (^{o}C) and H is relative humidity (%), can be a useful measure of fuel moisture content. Thus when a fire is burning in rugged terrain and montane fuels, we would suggest that in addition to the terrain conditions stipulated by the terrain-filter model, fire weather conditions satisfying $T - H \geq 35$ are also necessary for the fire channelling process to occur and have a significant affect on overall fire propagation.

The strength of the ambient winds will also be an important factor in determining whether channelling-driven fire spread will occur. The formation of lee slope or separation eddies is much more likely when ambient wind speeds are high (Sharples et al., submitted). The analyses of Sharples et al. (submitted) suggests that the occurrence of channelling-driven fire spread becomes significantly more likely when the ambient wind speed is in excess of 25-30 km h^{-1}. Consideration of the minimum wind speed associated with the events in table 3 also suggests that winds in excess of ?? km h^{-1} are necessary for fire channelling to occur.

It is important to continue recording the evolution of large fires using line-scan and other airborne technology. Such data, as it comes to hand, can be used to further test and refine the model presented here. In fact, as controlled wildfire experiments are not feasible on such a scale, careful and coordinated aerial monitoring is one of the only means of formally documenting large fires. Successful application of the model to additional cases would further support the rationale given above. Development of physical models that couple mass transport with wind-terrain interaction and fire development could also be used to strengthen the conclusions drawn above and will be the subject of further work by the authors.

Channelling-driven fire behaviour has implications for fire management and for fire fighter safety. Fire channelling events are very efficient mechanisms for spreading a fire across a landscape and the intense fire behaviour associated with them increases the likelihood of a fire transitioning to a plume-driven phase (Chatto, 1999). For example, the Flea Creek event described above ultimately resulted in the formation of a large pyro-cumulonimbus that reached an altitude of approximately 15 km (Fromm et al., 2006).

Furthermore, the threat of rapid lateral spread to fire fighter safety is clear; unexpected lateral spread has lead to entrapment of fire fighters in past fatal incidents (Butler et al., 1998; 2003; Cheney et al., 2001). The lateral spread associated with fire channelling also has the effect of rapidly increasing the width of a fire front. Indeed, during the recent large fires in Santa Barbara, CA, an acting fire chief was quoted as saying "Early last night all hell broke loose. We saw the fire spread laterally across the top of the city and the fire front extend to almost five miles (8 km) now" (DiMizio, 2009). This description, and the spatial scales that are alluded to, are consistent with the channelling events described above (e.g. Broken Cart event).

The case for fire channelling during the Santa Barbara fires is also supported by aerial photography of the Jesusita Fire (5 May – 18 May 2009). Figure 9a shows part of the Jesusita fire that exhibits a pattern of fire spread consistent with fire channelling. In figure 9a the ambient wind direction can be deduced from the plume direction and is roughly indicated by an arrow. The other arrow indicates the direction of fire spread. Of particular note are the right flanks of the fire in figure 9a: two parts of the flank are burning intensely, creating darker smoke and vigorous convection columns. Both of these sections of the fire are burning on lee slopes (topographic slope is unknown). Overall the pattern of fire spread on the right flank of the fire in figure 9a is similar to the pattern of spread on the northern flank of the Broken Cart fire (see figure 6), where two cascading events are evident. The pattern of fire spread and the characteristics of the smoke plumes in figure 9a are very similar to those in figure 9b and figure 9c. Figure 9b is a photograph of the Blue Range event (18 January 2003) which shows darker smoke and more vigorous convection on the right flank emanating from a fire burning on a lee slope, while figure 9c shows the visual band of the line-scan data over the Bendora Dam fire. Again the right flank is characterised by significantly darker smoke and more intense convection.

These distinguishing characteristics of a channelling event provide a clear set of indicators for when a channelling event is underway. For lookouts posted to monitor fire development, the appearance of darker smoke and vigorous convection on the flank of a fire burning on a lee slope should trigger an immediate message to incident controllers, warning them of the potential for rapid escalation of the fire. This information coupled with output from the terrain-filter model can be used to better inform fall-back scenarios should a channelling event occur. Knowledge of the parts of the landscape most prone to channelling-driven fire spread can also be used to better inform fire managers on where to safely place personnel (especially lookouts) and can be used to better inform fuel management strategies. The model, which is easily implemented in a GIS platform, could be used to better identify regions prone to channelling processes and thereby assist in prioritising fuel reduction treatments, including prescribed burning. Careful management of fuel in channelling prone regions could significantly reduce the chances of a fire transitioning to a larger fire-size class, and hence the overall risk posed by a bushfire burning in rugged terrain and montane fuels.

Acknowledgements
This work was undertaken as part of the Bushfire CRC's HighFire Risk project. The support of the Bushfire CRC is acknowledged.

References

Barry, R. G., 1992. *Mountain weather and climate*. 2nd edition. Routledge, New York.

Butler, B.W., Bartlette, R.A., Bradshaw, L.S., Cohen, J.D., Andrews, P.L., Putnam, T., Mangan, R.J., Brown, H., 1998. Fire Behavior Associated with the 1994 South Canyon Fire on Storm King Mountain, Colorado. US Forest Service Research Paper RMRMS-RP-9.

Butler, B.W., Bartlette, R.A., Bradshaw, L.S., Cohen, J.D., Andrews, P.L., Putnam, T., Mangan, R.J., Brown, H., 2003. The South Canyon Fire Revisited: Lessons in Fire Behaviour. *Fire Management Today* 63(4), 77-84.

Byron-Scott, R.A.D., 1990. The effects of ridge-top and lee-slope fires upon rotor motions in the lee of a steep ridge. *Mathematical and Computer Modelling*, 13(12), 103-112.

Cook, R., Walker, A., Wilkes, S., 2006. Airborne fire intelligence. In: *Proceedings of the 13th Australasian Remote Sensing and Photogrammetry Conference*, 20-24 November 2006, Canberra.

Chatto, K., (Ed.), 1999. Development, behaviour, threat and meteorological aspects of a plume-driven bushfire in west-central Victoria: Berringa Fire February 25-26, 1995. Research Report No. 48. Fire Management, Department of Natural Resources and Environment.

Cheney, P., J. Gould, and L. McCaw, 2001: The dead-man zone: a neglected area of fire fighter safety. *Australian Forestry*, 64, 45-50.

DiMizio, A., 2009. Excerpt of press release. Andrew DiMizio, Santa Barbara Acting Fire Chief. ABC TV News, 9 May 2009.

Dold, J., Weber, R.O., Gill, A.M., Ellis, P., McRae, R., Cooper, N., 2005. Unusual Phenomena in an Extreme Bushfire. In: *Proceedings of the 5th Asia-Pacific Conference on Combustion*, 17-20 July 2005, The University Adelaide, South Australia.

Doran, J.C., Whiteman, C.D., 1992. The coupling of synoptic and valley winds in the Tennessee valley. In: *Proceedings of the 6th conference on mountain meteorology*. American Meteorological Society, Boston.

Farr, T.G., Rosen, P.A., Caro, E., Crippen, R., Duren, R., Hensley, S., Kobrick, M., Paller, M., Rodriguez, E., Roth, L., Seal, D., Shaffer, S., Shimada, J., Umland, J., Werner, M., Burbank, D., Alsdorf, D., 2007. The Shuttle Radar Topography Mission. *Reviews of Geophysics*, 45, RG2004, doi: 10.1029/2005RG000183.

Fiedler, F., 1983. Einige characteristika der strömungen im oberrheingraben. *Wissenschaftliche Berichte des Meteorologischen Instituts der Universität Karlsruhe*, 4, 113-123.

Fromm, M., Tupper, A., Rosenfeld, D., Servranckx, R., McRae, R., 2006. Violent pyro-convective storm devastates Australia's capital and pollutes the stratosphere, *Geophysical Research Letters* 33, L05815

Gross, G., Wippermann, F., 1987. Channelling and countercurrent in the upper Rhine valley: numerical simulations. *Journal of Climate and Applied Meteorology*, 26, 1293-1304.

Harrison, B.A., Jupp, D.L.B., 1989. *Introduction to remotely sensed data*. CSIRO Australia.

Kossman, M., Sturman, A.P., 2002. Dynamic airflow channelling effects in bent valleys. In: *Proceedings of the 10th conference on mountain meteorology.* 17-21 June 2002, Park City UT. American Meteorological Society.

Kossman, M., Sturman, A.P., 2003. Pressure-driven channelling effects in bent valleys. *Journal of Applied Meteorology*, 42(1), 151-158.

Kossmann, R., Sturman, A. & Zawar-Reza, P., 2001., *Atmospheric influences on bush fire propagation and smoke dispersion over complex terrain.* Proceedings, 2001 Australasian Bushfire Conference, Christchurch NZ.

Lee, J.T., Barr, S., Snyder, W.H., Lawson, R.E. Jnr., 1981. Wind tunnel studies of flow channelling in valleys. In: *Proceedings of the 2nd conference on mountain meteorology.* 9-12 November 1981. Steamboat Springs CO. American Meteorological Society.

McRae, R., 2004. Breath of the dragon – observations of the January 2003 ACT Bushfires. In: *Proceedings of 2004 Australasian Bushfire Research Conference*, May 2004, Adelaide.

McRae, R. 1997. Considerations on operational wildfire spread modelling. In: *Proceedings, Bushfire 1997. Australian Bushfire Conference*, July 1997, Darwin.

Mills, G.A., 2006. On the sub-synoptic scale meteorology of two extreme fire weather days during the Eastern Australian fires of January 2003. *Australian Meteorological Magazine* 54, 265-290.

Mitchell, R. M., D.M. O'Brien & S.K. Campbell (2006. Characteristics and radiative impact of the aerosol generated by the Canberra firestorm of January 2003. *Journal of Geophysical Research* 111, D02204

Nairn, G. (Chair), 2003. *A Nation Charred: Inquiry into the Recent Australian Bushfires*. The Parliament of the Commonwealth of Australia, Canberra.

Papadopoulos, K.H., Helmis, C.G., Amanatidis, G.T., 1992. An analysis of wind direction and horizontal wind component fluctuations over complex terrain. *Journal of Applied Meteorolgy*, 31, 1033-1040.

Rothermel, R.C., 1993. Mann Gulch Fire: A Race That Couldn't Be Won. US Forest Service General Technical Report INT-299. May 1993.

Rothermel, R.C., Brown, H., 2003. A Race That Couldn't Be Won. *Fire Management Today*, 63(4),75-76.

Rothermel, R.C., Mutch R.W., 2003. Behaviour of the Life-Threatening Butte Fire: August 27-29, 1985. *Fire Management Today*, 63(4), 31-39.

Sharples, J.J., McRae, R.H.D., Weber, R.O., Gill, A.M., 2009. A simple index for assessing fuel moisture content. *Environmental Modelling and Software*, 24, 637-646.

Sharples, J.J., in press. An overview of mountain meteorological effects relevant to fire behaviour and bushfire risk. *International Journal of Wildland Fire*

Smedman, A.-S., Bergström, H., Högström, U., 1996. Measured and modelled local wind fields over a frozen lake in a mountainous area. *Contributions to Atmospheric Physics*, 69, 501-516.

Taylor, J., Webb, R., 2005. Meteorlogical aspects of the January 2003 south-eastern Australian bushfire outbreak. *Australian Forestry* 68(2).

Taylor, J.R., Kossmann, M., Low, D.J., Zawar-Reza, P., 2005. Summertime easterly surges in southeastern Australia: a case study of thermally forced flow. Australian Meteorological Magazine, 54, 213-223.

Webb, R., Davis, C. and Lleyett, S., 2004. Meteorological aspects of the ACT bushfires of January 2003. Proceedings of the Conference *Bushfire 2004: Earth, Wind and Fire - Fusing the Elements.* South Australian Department of Environment and Heritage, Adelaide, South Australia.

Weber, R.O., Kauffmann, P., 1998. Relationship of synoptic winds and complex terrain flows during the MISTRAL field experiment. *Journal of Applied Meteorology*, 37, 1486-1496.

Whiteman, C.D., Doran, J.C., 1993. The relationship between overlying synoptic-scale flows and winds within a valley. *Journal of Applied Meteorology*, 32, 1669-1682.

Wippermann, F., 1984. Air flow over and in broad valleys: channelling and counter-current. *Contributions to Atmospheric Physics*, 57, 92-105.

Wippermann, F., Gross, G., 1981. On the constriction of orographically influenced wind roses for given distributions of the large-scale wind. *Bietraege zur Physik der Atmosphere*, 54, 492-501.

Whiteman, C.D., 2000. *Mountain Meteorology: Fundamentals and Applications*. Oxford University Press.

Table and Figure Captions

Table 1. Description of the spectral bands of the Daedalus 1268 ATM device, their characteristics and uses**.**

Table 2. Indicative RGB coordinate values for features in images with well balanced pixel intensity distribution.

Table 3. Catalogue of fire channelling events. All events have been identified as channelling events through analyses of multispectral line-scan data or aerial photography. All events are in southeastern Australia, except for the Esperanza and Jesusita events which occurred in California. Type 'V' indicates that the event occurred in connection with an incised valley, while 'L' indicates that the event occurred in connection with a lee slope.

Figure 1. Wind speed (grey lines), gust (black lines) and direction (boxes) data recorded at (a) Canberra Airport and (b) Curtin Emergency Services Bureau Headquarters on 18 January 2003.

Figure 2. (a) Map of southeastern Australia showing the locations of events considered in the study, (b) Map showing the locations of the Flea Creek, Broken Cart and Bendora Dam events in relation to the main geographic features and topography of the region.

Figure 3. Multispectral line-scan data for the Bendora Fire overlayed on DEM data (100 m contours). (a) Bendora Dam event imaged at 14:46 [Run 2], (b) Bendora Dam event imaged at 15:32, clearly moving southwards [Run 6]. The circled region in (a) is where the fire reignited. The arrow in (a) indicates the ambient wind direction.

Figure 4. Multispectral line-scan data for the McIntyres Hut Fire overlayed on DEM data (100 m contours). (a) Flea Creek part of the McIntyres Hut Fire imaged at 15:13 [Run 4], (b) Flea Creek part of the McIntyres Hut Fire imaged at 15:22 [Run 5]. The arrow in (a) indicates the ambient wind direction.

Figure 5. Multispectral line-scan data for the Broken Cart Fire overlayed on DEM data (100 m contours). (a) Broken Cart Fire imaged at 15:03 [Run 3], and (b) Broken Cart Fire imaged at 15:09 [Run 4]. The arrow in (a) indicates the ambient wind direction.

Figure 6. Example of output from the model (equation (1)) for identifying channelling prone parts of the landscape (indicated in grey). Thin black lines are 10-minute isochrones of the Broken Cart Fire derived from the line-scan data, showing the influence of three events (outlined) on lateral spread. The model was applied assuming $\theta_w = 112.5^o$ and parameter values of $\sigma = 10.5^o$ and $\delta = 33^o$.

Figure 7. Fire channelling events at Thredbo, 26 January 2003. The contour interval is 50m with emphasis on the 1500m contour. (a) Multispectral line-scan data overlayed on DEM contours with hill-shading, (b) Semi-transparent rendering of the line-scan data

overlayed on DEM contours and regions identified by the terrain-filter model. Wind direction was taken to be ???? (indicated by the arrow in panel (a)). The model parameters are assumed to have the same values as derived during the calibration of the model.

Figure 8. Schematic diagrams illustrating the hypothetical mechanisms suggested by the modelling results. (a) fire channelling along an incised valley, (b) fire channelling across a lee slope.

Figure 9. Fire channelling events. (a) Two apparent channelling events underway during the Jesusita Fire, Santa Barbara May 2009 (image taken from ABC TV News 9 May 2009). (b) The Blue Range (west of Canberra) event underway, 18 January 2003 (photograph taken by S. R. Wilkes). (c) The Bendora Dam channelling event underway (image taken from line-scan visual band: 15:32 [Run 6], see figure 3b). In all images note the darker smoke and vigorous convection on the right flank in the lee of the ridge lines. The arrows indicate the ambient wind direction and the lateral direction of spread

Tables and Figures

Table 1.

Daedalus 1268 ATM Spectral Band Properties				
Band	**Wavelength Range**	**Spectrum**	**Characteristics**	**Use**
1	420 – 450 nm	—	Substantially influenced by atmospheric scattering	—
2 (TM1)	450 – 520 nm	Blue	Lower wavelength cut off below peak transmittance of clear water. Upper cut off limit of blue chlorophyll absorption	Penetration of water bodies, discriminating soil and vegetation characteristics
3 (TM2)	520 – 600 nm	Green	Spans region between blue and red chlorophyll absorption	Green reflectance of healthy vegetation
4	605 – 625 nm	—	—	—
5 (TM3)	630 – 690 nm	Red	Includes the chlorophyll absorption of healthy vegetation	Most important band for vegetation discrimination
6	695 – 750 nm	—	—	—
7 (TM4)	760 – 900 nm	Near Infrared	Reflective infrared radiation	Responsive to amount of vegetation biomass on surface
8	910 – 1050 nm	Near Infrared	—	—
9 (TM5)	1.55 – 1.75 µm	Mid Infrared	Sensitive to the turgidity of plants (water content)	Can discriminate between cloud, snow and ice
10	2.08 – 2.35 µm	Mid Infrared	—	—
11 (TM6) High Gain	8.5 – 13.0 µm	Thermal Infrared	Infrared radiant flux from surfaces	Apparent temperature of surface, geothermal indication, vegetation classification and stress analysis
12 (TM6) Low Gain	8.5 – 13.0 µm	Thermal Infrared	Infrared radiant flux from surfaces	Apparent temperature of surface, geothermal indication, vegetation classification and stress analysis
13	INS Data	—	Geographic position, aircraft roll, pitch and yaw for each scan line	First order georectification

Table 2. Description of the spectral bands of the Daedalus 1268 ATM device, their characteristics and uses**.**

Table 2.

Feature	Pseudocolour	R	G	B	Variants
Flame	Yellow	255	255	0	Tends to be at saturation.
Flaming zone	Bright orange	120	200	0	Intensity varies with time since ignition.
Cooling	Dark orange	120	120	0	Speed of cooling depends on the amount of large (slow burning) fuel.
Burnt but cool	Dark burgundy	90	60	0	Varies with terrain shading.
Unburnt forest	Dark green-brown	60	60	0	Varies with terrain shading.
Unburnt grassland	Light green	240	190	0	Varies with terrain shading and shrub density.
Shadow of dense smoke	Dark red	90	30	0	Varies with density – largely a modifier to vegetation signature.
Superheated gas	Pale blue	20	240	240	Tends to be distorted due to proximity to scanning sensor.
Superheated gas over flame	White	255	255	255	
Water (reflection)	Light blue	0	255	255	Farm dams or large pools in rivers.
Water (dark)	Black	0	0	0	Most water surfaces – no reflection to the sensor.
Dense smoke	Various	~	~	0 to 150	As it is transparent in R and G, some B is added to the prior signature.

Table 2. Indicative RGB coordinate values for features in images with well balanced pixel intensity distribution.

Table 3.

Date	Location	Longitude (d.dd°)	Latitude (d.dd°)	Elevation (m)	Type
6 Dec 2002	Fiddletown	151.07	-33.60	200	V
18 Jan 2003	Flea Creek	148.73	-35.28	600	V
	Pig Hill	148.88	-35.23	1000	V
	Dingo Dell	148.84	-35.26	1000	V
	Hyles Block South	148.94	-35.26	500	V
	Genges Trig.	148.85	-35.27	1100	L
	Blue Range	148.86	-35.29	1100	L
	Cotter Reserve	148.95	-35.31	600	L
	Brindabella Road Lower	148.76	-35.38	800	L
	Brindabella Road Upper	148.78	-35.38	1000	L
	Bendora Dam	148.82	-35.45	900	V
	Cooleman Creek (Broken Cart)	148.70	-35.45	900	L
	Browns Creek (Broken Cart)	148.65	-35.46	900	L
	Log Hut Creek (Broken Cart)	148.65	-35.52	1300	L
	Orroral Valley	148.99	-35.68	1100	L
26 Jan 2003	“Kenya” property	148.75	-35.16	1000	V
	Burrungubugge River	148.48	-36.25	1700	V
	Guthega	148.38	-36.37	600	V
	Thredbo #1	148.39	-36.45	1400	V
	Thredbo #2	148.43	-36.43	1500	V
	Thredbo #3	148.46	-36.41	1500	V
	Thredbo #4	148.55	-36.38	1200	V
	Dead Horse Gap	148.35	-36.53	1700	L
	Tom Groggin	148.13	-36.59	900	L
26 Oct 2006	Esperanza Fire, CA	116.86	33.84	1200	L
5 May 2009	Jesusita Fire, CA	119.7	34.4	200	L

Table 3. Catalogue of fire channelling events. All events have been identified as channelling events through analyses of multispectral line-scan data or aerial photography. All events are in southeastern Australia, except for the Esperanza and Jesusita events which occurred in California. Type ‘V’ indicates that the event occurred in connection with an incised valley, while ‘L’ indicates that the event occurred in connection with a lee slope.

Figure 1.

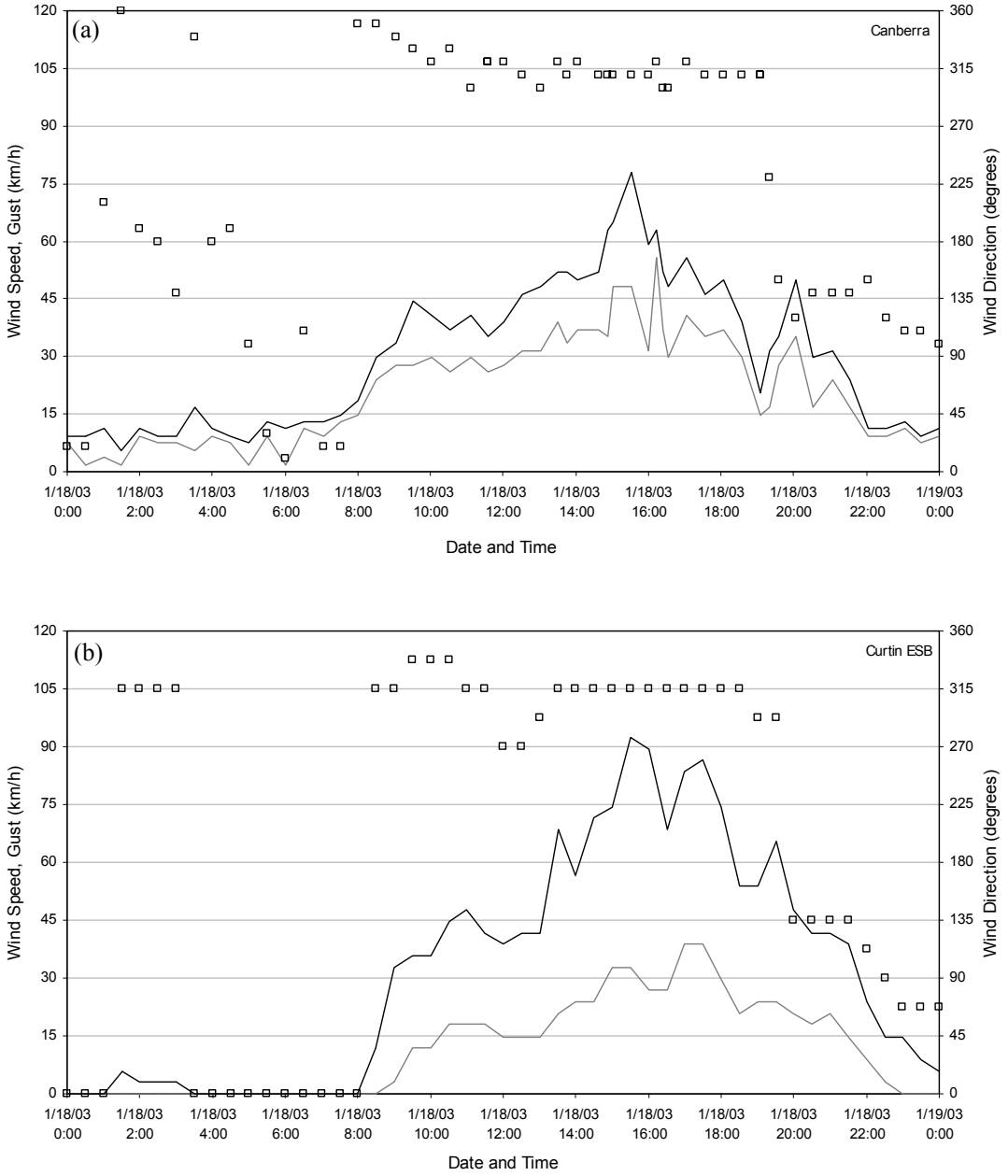

Figure 1. Wind speed (grey lines), gust (black lines) and direction (boxes) data recorded at (a) Canberra Airport and (b) Curtin Emergency Services Bureau Headquarters on 18 January 2003.

Figure 2.

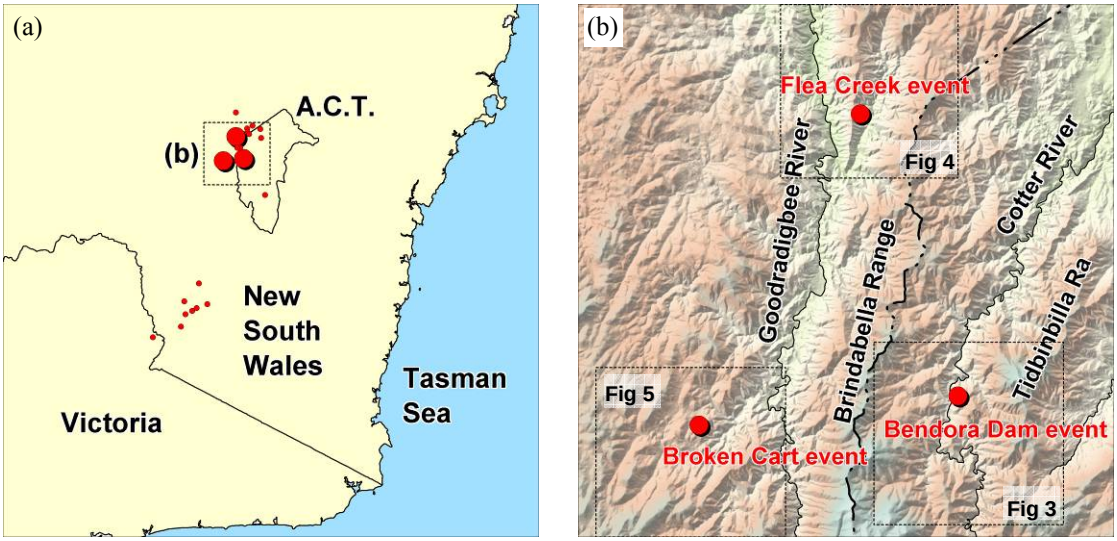

Figure 2. (a) Map of southeastern Australia showing the locations of events considered in the study, (b) Map showing the locations of the Flea Creek, Broken Cart and Bendora Dam events in relation to the main geographic features and topography of the region.

Figure 3.

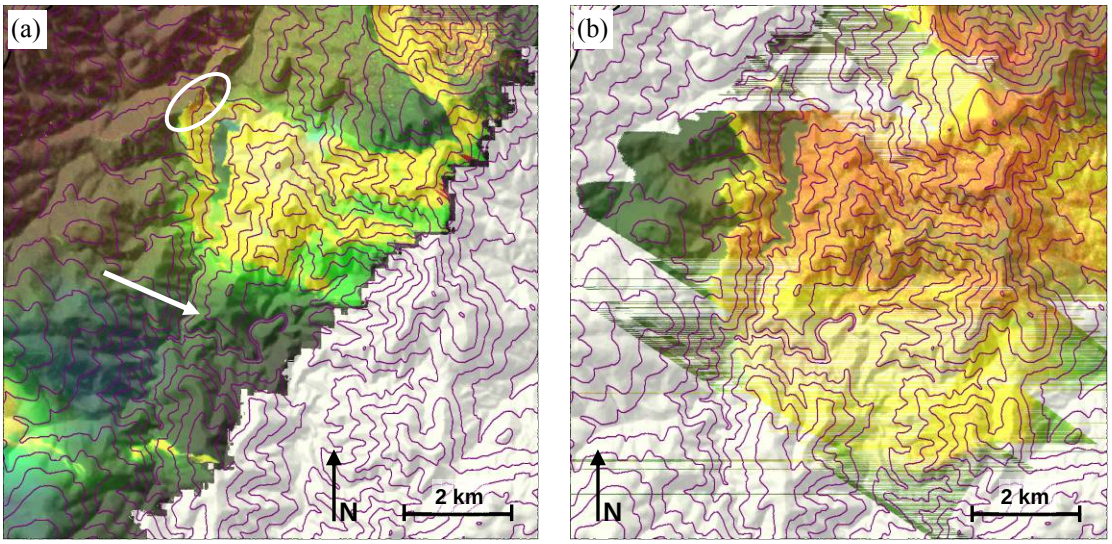

Figure 3. Multispectral line-scan data for the Bendora Fire overlayed on DEM data (100 m contours). (a) Bendora Dam event imaged at 14:46 [Run 2], (b) Bendora Dam event imaged at 15:32 [Run 6], clearly moving southwards. The circled region in (a) is where the fire reignited. The arrow in (a) indicates the ambient wind direction

Figure 4.

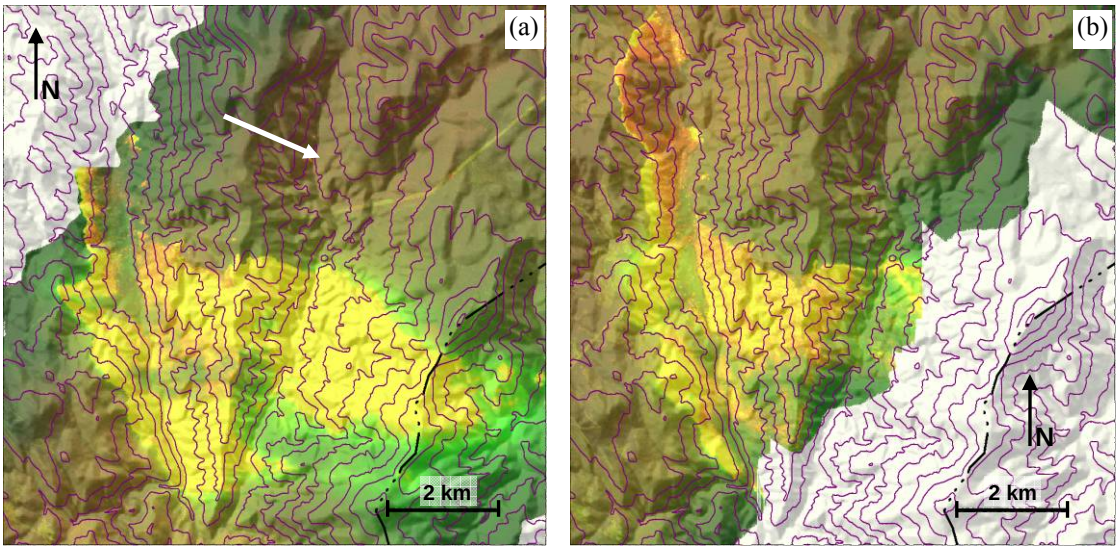

Figure 4. Multispectral line-scan data for the McIntyres Hut Fire overlayed on DEM data (100 m contours). (a) Flea Creek – Goodradigbee River part of the McIntyres Hut Fire imaged at 15:13 [Run 4], (b) Flea Creek – Goodradigbee River part of the McIntyres Hut Fire imaged at 15:22 [Run 5]. The arrow in (a) indicates the ambient wind direction

Figure 5.

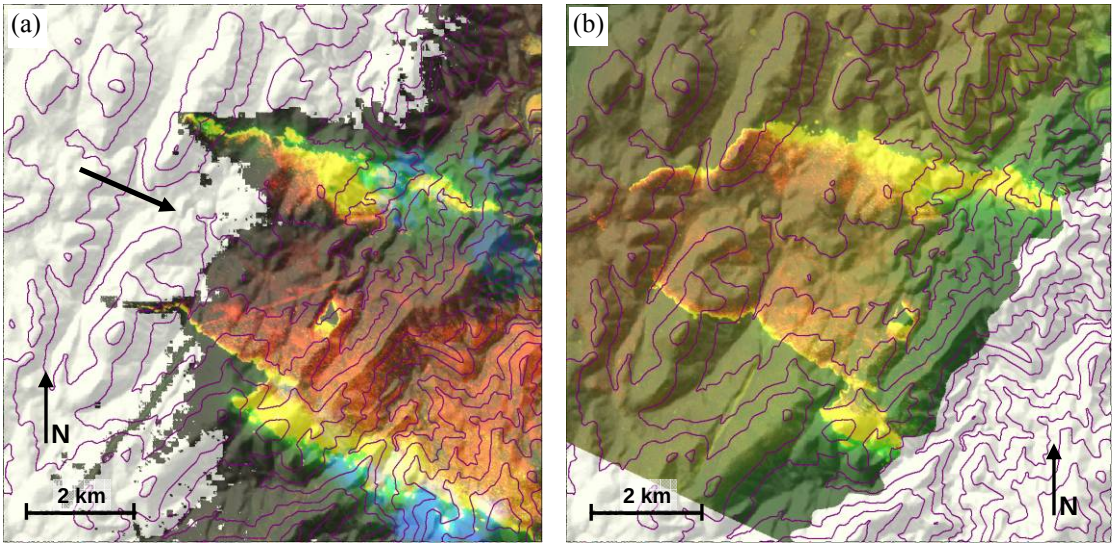

Figure 5. Multispectral line-scan data for the Broken Cart Fire overlayed on DEM data (100 m contours). (a) Broken Cart Fire imaged at 15:03 [Run 3], and (b) Broken Cart Fire imaged at 15:09 [Run 4]. The arrow in (a) indicates the ambient wind direction

Figure 6.

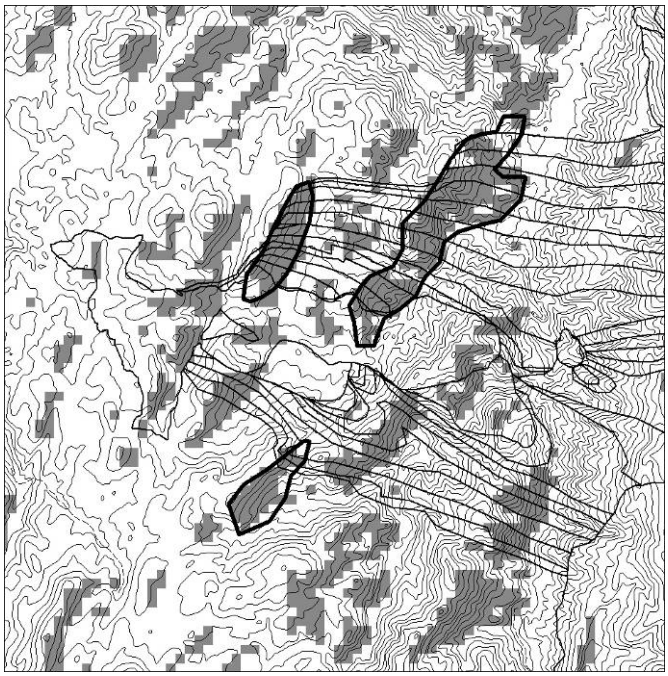

Figure 6. Example of output from the model (equation (1)) for identifying channelling prone parts of the landscape (indicated in grey). Thin black lines are 10-minute isochrones of the Broken Cart Fire derived from the line-scan data, showing the influence of three events (outlined) on lateral spread. The model was applied assuming $\theta_w = 112.5^o$ and parameter values of $\sigma = 10.5^o$ and $\delta = 33^o$.

Figure 7.

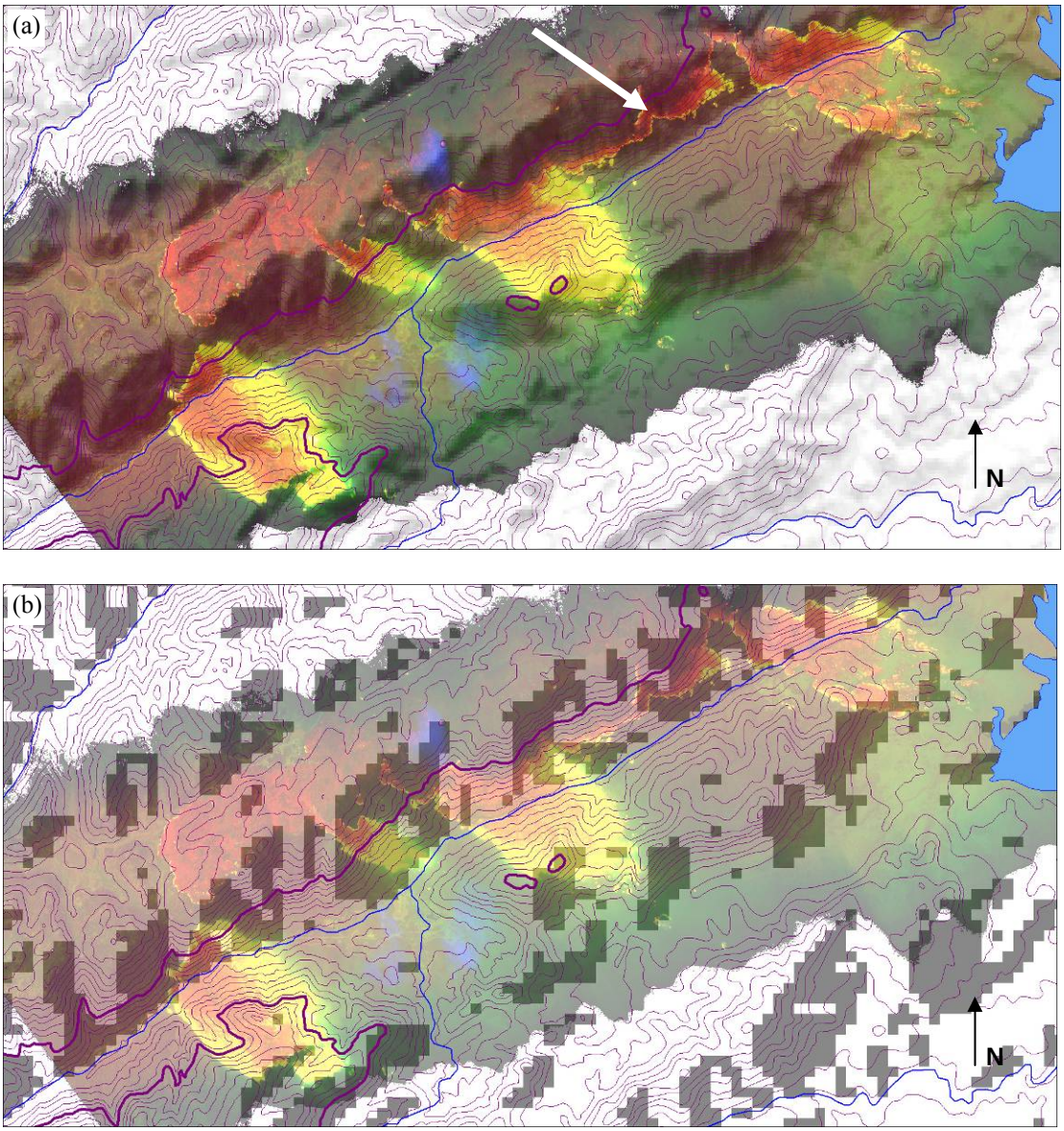

Figure 7. Fire channelling events at Thredbo, 26 January 2003. The contour interval is 50m with emphasis on the 1500m contour. (a) Multispectral line-scan data overlayed on DEM contours with hill-shading, (b) Semi-transparent rendering of the line-scan data overlayed on DEM contours and regions identified by the terrain-filter model (grey grid cells). Wind direction was taken to be ???? (indicated by the arrow in panel (a)). The model parameters are assumed to have the same values as derived during the calibration of the model.

Figure 8.

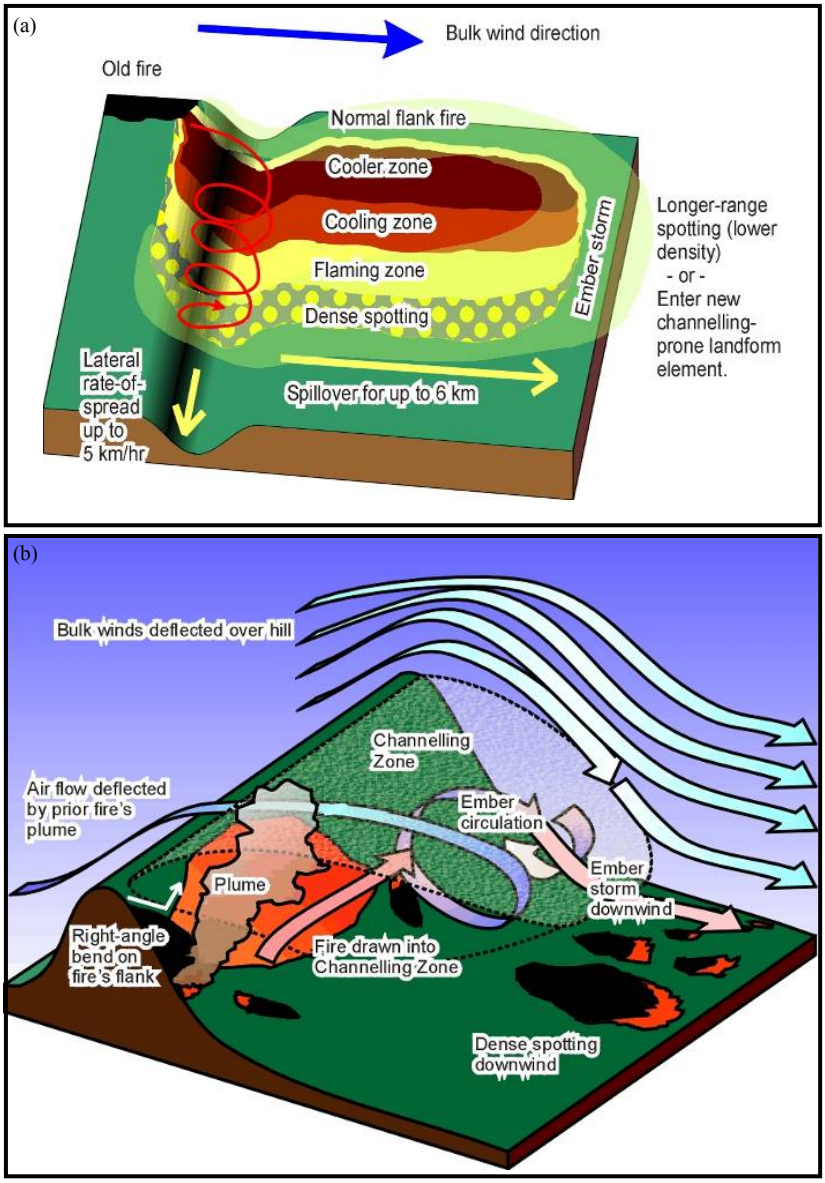

Figure 8. Schematic diagrams illustrating the hypothetical mechanisms suggested by the modelling results. (a) fire channelling along an incised valley, (b) fire channelling across a lee slope.

Figure 9.

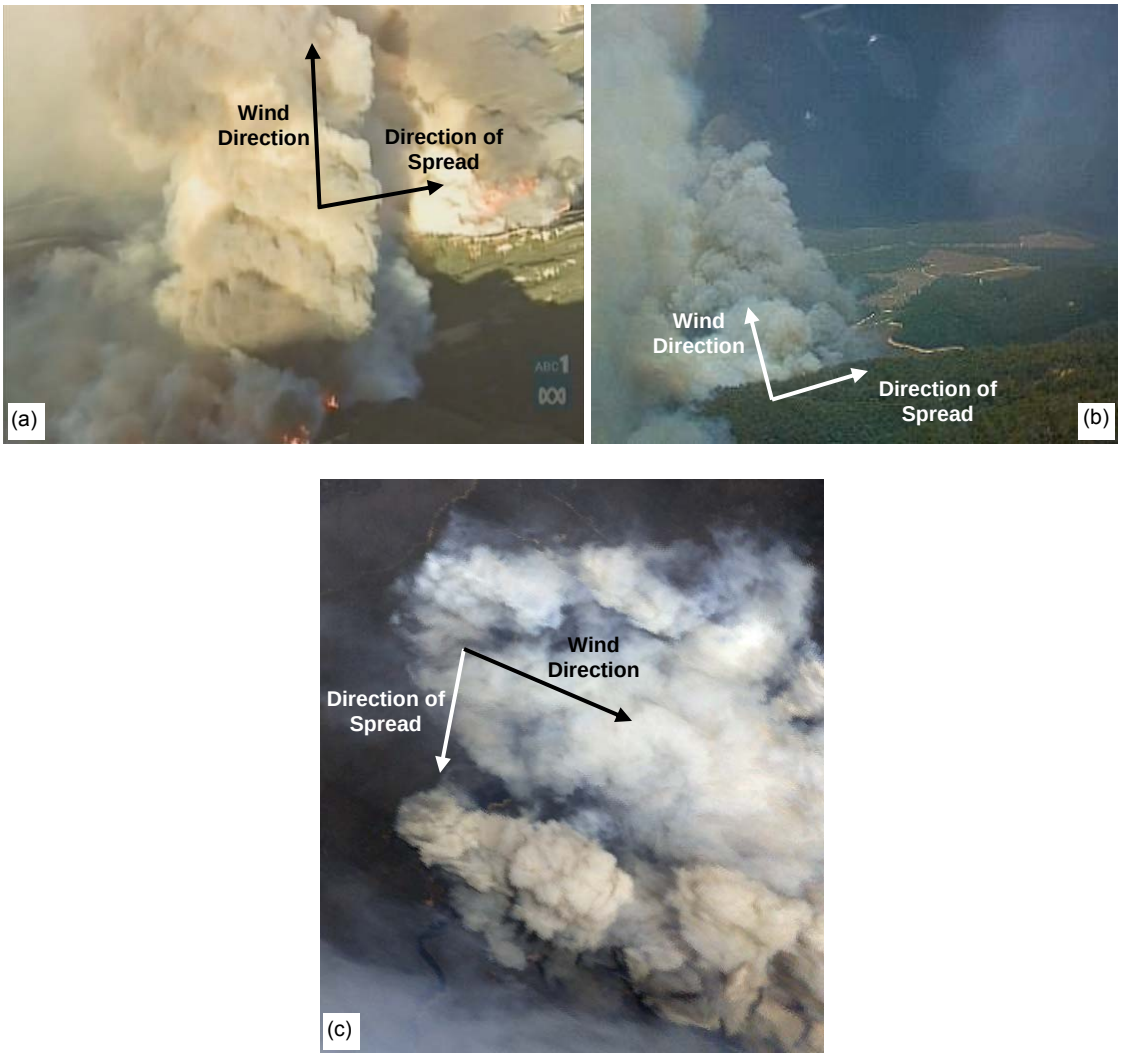

Figure 9. Fire channelling events. (a) Two apparent channelling events underway during the Jesusita Fire, Santa Barbara May 2009 (image taken from ABC TV News 9 May 2009). (b) The Blue Range (west of Canberra) event underway, 18 January 2003 (photograph taken by S. R. Wilkes). (c) The Bendora Dam channelling event underway (image taken from line-scan visual band: 15:32 [Run 6], see figure 3b). In all images note the darker smoke and vigorous convection on the right flank in the lee of the ridge lines. The arrows indicate the ambient wind direction and the lateral direction of spread